

Modeling HIV infection dynamics: a comparative analysis of four viral dynamics models

Alberto Catalano, Anna Salsano

Abstract

This report provides a comparative analysis of four mathematical models used to simulate the dynamics of Human Immunodeficiency Virus (HIV) infection. Utilizing systems of ordinary differential equations (ODEs), the study explores the within-host interactions between viral replication, target cell depletion and host immune responses. Initial simulations using the basic model for viral dynamics capture the fundamental features of the acute infection phase and the establishment of a chronic viral set-point. To increase biological realism, subsequent models incorporate latent reservoirs and a dual infection pathway involving both cell-free and cell-to-cell transmission. The inclusion of cell-mediated and humoral immunity further shows how cytotoxic T lymphocytes and neutralizing antibodies jointly restrict viral spread. A high-fidelity complex model is then presented, which integrates thymic development and viral tropism switching to replicate the triphasic progression of the disease. This comprehensive framework successfully reproduces clinically observed phenomena, such as the characteristic double viral peak during the acute phase. Simulations conducted in Matlab demonstrate that the initiation of antiretroviral therapy (ART) triggers exponential viral decay and facilitates robust immune reconstitution. The results emphasize the role of latent reservoirs in preventing total viral eradication. Ultimately, these predictive models provide a quantitative framework for assessing therapeutic efficacy and the long-term clinical outcomes of HIV infection.

I. INTRODUCTION

Since it was first characterized as a novel virus in the 1980s, **Human Immunodeficiency Virus (HIV)**, responsible for acquired immunodeficiency syndrome (AIDS), has emerged as one of the most devastating pandemics in modern history, infecting approximately 91 million people and causing around 44 million deaths, according to World Health Organization statistics as of 2024. Nevertheless, thanks to advances in antiretroviral therapy (ART), annual deaths from HIV have declined from 1.3 million in 2010 to 650 000, with ART now reaching approximately 75% of people living with HIV [1].

Biologically classified as a *Lentivirus*, HIV replicates through error-prone reverse transcription, a process that generates **high genetic diversity**, which complicates personalized treatment and creates significant challenges for both drug resistance and vaccine development [2]. The virus is primarily transmitted sexually, but it can also spread through maternal-infant transmission, percutaneous exposure and contact with infected blood. After transmission, HIV initially establishes infection in mucosal tissues before spreading to lymphoid organs. The virus primarily targets **CD4+ cells**, including T lymphocytes, monocytes, macrophages and dendritic cells. Infected cells produce new virions, further propagating the infection.

As plotted in *Figure 1*, HIV infection progresses through four phases [3]:

- **Eclipse phase:** asymptomatic phase that begins immediately after transmission, during which the virus infects initial cells and spreads to lymph nodes. This phase typically lasts up to three weeks.
- **Acute phase:** plasma HIV-RNA levels peak (up to 10^6 copies/mL) before declining due to host immune responses. Seroconversion occurs, marked by the appear-

ance of detectable HIV antibodies. This phase can last from several days to weeks.

- **Clinical Latency:** a viral set point is established, CD4+ T cell counts gradually decline and infection progresses slowly toward AIDS if untreated. Chronic inflammation, particularly in lymphoid tissues, is common, and plasma HIV-RNA levels typically range in the thousands of copies per mL.
- **AIDS:** marked by high viremia and severe CD4+ T cell depletion, the immune system becomes compromised, leading to opportunistic illnesses.

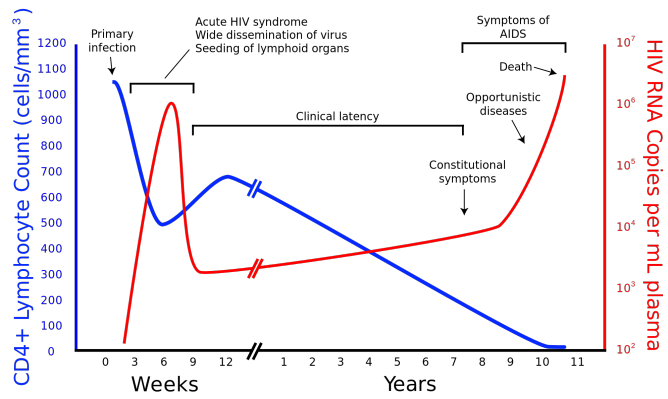


Fig. 1. *Dynamics of HIV progression from infection to AIDS* [4]. The graph shows the inverse relationship between CD4+ T lymphocyte count (blue, left axis) and plasma HIV RNA viral load (red, right axis) in an untreated individual. The timeline illustrates the progression from acute infection (weeks) through clinical latency to the terminal phase (years).

HIV infection triggers both humoral and cell-mediated immune responses. Cytotoxic T lymphocytes (CTLs) play a

central role in controlling viral replication by recognizing and eliminating infected cells [5], while **antibodies** generated by the humoral response can neutralize free virus and limit its spread [6]. Despite these defenses, HIV persists by evading immune surveillance through strategies such as **cell-to-cell** transmission and the establishment of latent viral reservoirs.

Given the complexity of HIV infection and the host immune response, the development of predictive **mathematical models** provides a valuable framework to quantitatively assess interpatient variability, as well as the efficacy and potential toxicity of different treatment strategies on disease progression. That's the reason why HIV has been extensively studied using mathematical models, ranging from simple frameworks to highly complex representations of **viral dynamics and immune interactions** [7].

Mathematical modelling translates complex systems (such as virus-host interactions, as in this report) into formal languages to analyze their behavior and make predictions [8]. Different levels of abstraction exist:

- **Qualitative Models** (Logic Modelling): these employ Boolean algebra (0/1, active/inactive) to describe regulatory networks without requiring detailed kinetic parameters.
- **Quantitative Models** (ODE and Stochastic): These are used when kinetic data (reaction rates, concentrations) are available and mass-action law based approaches can be applied. In particular, the **deterministic** approaches based on **ODE** have these features and limitations:
 - **Continuum Hypothesis:** ODE models assume molecular or cellular populations are sufficiently large that random fluctuations (biological noise) can be neglected, allowing variables to be treated as continuous concentrations.
 - **Mean Dynamics:** Deterministic simulations compute the mean temporal evolution of the system. While computationally efficient, they may deviate from biological reality when population sizes are small, in which case stochastic simulation algorithms (SSA) are more appropriate.
 - **Numerical Solution:** The models are solved numerically using methods such as Euler or Runge–Kutta schemes, which discretize time with step size h to approximate state derivatives.

A crucial aspect of a mathematical model is **parameter estimation**. Viral models require parameters that are often not directly measurable. So in this case, the parameter calibration constitutes a **Dynamical Inverse Problem** (or reverse engineering): instead of computing the dynamics given a model, one aims to derive the model's structure and parameters by observing experimental dynamics data. This process is fundamental for transforming a qualitative network into a predictive quantitative model.

In this report we present and provide a Matlab implementation of four HIV models originally grouped and described by A. V. Rodriguez et al. [9], further expanding them with the study of

ART dynamics. We begin with the **basic HIV viral dynamics model** (*Section II* - [10]), which will be the basis of the models that were implemented in this report. We then progressively increase the complexity by incorporating additional elements critical to HIV dynamics, including **cell-to-cell transmission** (*Section III* - [11]) and both cell-mediated and humoral **immune responses** (*Section IV* - [12]), culminating with the **most comprehensive model** proposed in the original work (*Section V* - [13]).

These models belong to HIV within-host dynamics, they all use ODEs to describe different phases of infection and the effect of ART therapy.

II. BASIC HIV VIRAL DYNAMICS MODEL

The Basic Viral Dynamics model, originally developed by Nowak and May, represents the foundational mathematical approach for describing HIV infection and the effects of treatment. This model serves as a **starting point** for more complex variations by tracking the levels of three primary components: uninfected CD4+ T cells (T), the free virus (V) and infected T cells (I) [10]. The schematic representation of the model is illustrated in *Figure 2*.

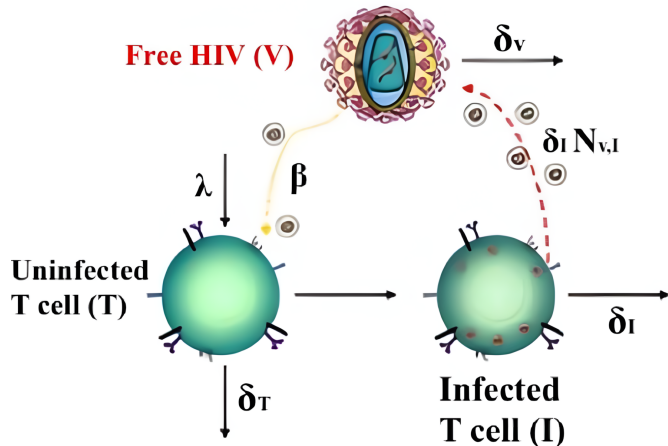


Fig. 2. The diagram illustrates the interactions between uninfected CD4+ T cells (T), infected cells (I), and free virus (V), each controlled by specific parameters.

The parameters governing the interactions between the cell populations and the virus are detailed in *Table I*. The values presented are specific to the simulation implemented in the provided code. The system is governed by the constant production of target cells (λ), the infection rate (β), viral production from infected cells ($N_{v,I}$), and the specific death or clearance rates (δ) for each population.

The dynamics of the system are described by the following set of ODEs:

$$\frac{dT}{dt} = \lambda - \delta_T T - (1 - \epsilon) \beta V T \quad (1)$$

$$\frac{dI}{dt} = (1 - \epsilon) \beta V T - \delta_I I \quad (2)$$

$$\frac{dV}{dt} = \rho I - \delta_V V \quad (3)$$

TABLE I
Parameters for the Basic HIV Viral Dynamics Model

Param.	Description	Value	Units
λ	Production rate of T-cells	10,000	cells day ⁻¹
β	Infectivity rate	8×10^{-7}	mL copies ⁻¹ day ⁻¹
δ_T	Natural death rate of healthy T-cells	0.01	day ⁻¹
δ_I	Death rate of infected T-cells	0.7	day ⁻¹
$N_{v,I}$	Virions produced per infected cell	100	virions cell ⁻¹
δ_V	Viral clearance rate	23	day ⁻¹
ϵ	Therapy efficacy (when active)	0.9	–

The mathematical formulation presented explicitly incorporates the effect of ART by modifying the infection term. Specifically, the infectivity rate β is scaled by a factor of $(1-\epsilon)$, where ϵ represents the drug efficacy; in scenarios where no treatment is active, ϵ is set to 0, reverting the system to the standard untreated dynamics.

The first equation describes the rate of change of uninfected T cells, which is determined by the balance between the natural supply of new cells and their depletion due to natural turnover and viral infection.

The second equation tracks the population of infected T cells, representing the accumulation of newly infected cells driven by the interaction between virus and healthy cells, balanced against their removal caused by cell death.

The third equation defines the dynamics of the free viral load, driven by the continuous release of virions from infected cells and offset by the clearance of viral particles from the system.

Having established the mathematical framework and defined the parameters, we now proceed to the **simulation** of the system to visualize the dynamics of the infection.

The simulation of the basic model without therapeutic intervention (*Figure 3*) effectively reconstructs the dynamics of the **acute phase** of HIV infection.

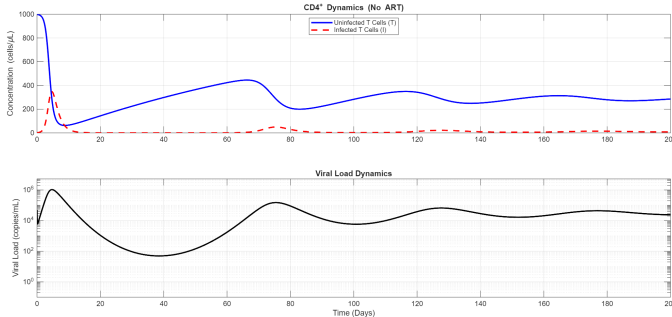


Fig. 3. **Simulation of Untreated HIV Infection.** The top panel illustrates the cellular dynamics over time (days), where the blue solid line represents the concentration of uninfected CD4+ T cells and the red dashed line shows the infected T cells (cells/ μ L). The bottom panel displays the corresponding viral load in copies/mL on a logarithmic y-axis.

Following the introduction of the virus ($t = 0$), the viral load exhibits rapid exponential growth, peaking at levels exceeding

10^6 copies/mL within the first few weeks. This viral peak causes a decline in the uninfected CD4+ T cell population, that crashes from an initial condition of 1000 cells/ μ L to levels below 100 cells/ μ L. Following this acute phase, the viral load decreases as virus target cells become scarce. The system then enters a phase of damped oscillations, before settling into a **quasi-steady state** characterized by a chronically high viral load and a stable, yet significantly depleted, CD4+ T cell count of approximately 200 cells/ μ L.

The application of ART is simulated starting at day 200, with an efficacy of 90% (*Figure 4*). Upon the administration of ART the viral load undergoes a sharp exponential decay, dropping to zero within weeks. As a consequence of this viral suppression, the uninfected CD4+ T cell population begins an immediate recovery, rising to over 600 cells/ μ L by day 300, and returning to the starting concentration by approximately day 500, demonstrating the potential for immune reconstitution under effective suppressive therapy.

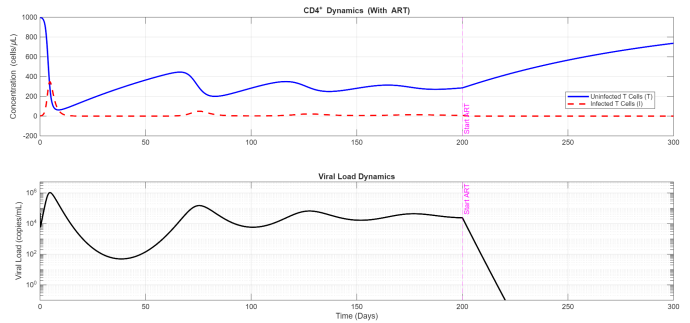


Fig. 4. **Simulation of HIV Dynamics with ART Intervention.** The top panel tracks T-cell populations (y-axis: cells/ μ L) over 300 days, showing the recovery of uninfected T cells (blue solid line) and the decline of infected T cells (red dashed line). The bottom panel depicts the viral load, which drops exponentially following the initiation of ART, marked by the vertical magenta dashed line at day 200.

The Basic Viral Dynamics model successfully explains the fundamental interaction between HIV and CD4+ T cells, capturing the key features of acute infection (viral peak and CD4+ depletion) and the establishment of a stable chronic infection. It also correctly predicts the correlation between viral suppression and CD4+ recovery upon treatment initiation.

However, the model exhibits notable **limitations** regarding the complexity of long-term disease progression and therapeutic response. Primarily, it predicts a purely monophasic viral decline following treatment, contradicting clinical data which typically show a biphasic decay driven by long-lived cell populations and latent reservoirs. Consequently, the model incorrectly suggests that perfectly effective therapy leads to total viral extinction, failing to account for the viral persistence that renders complete eradication impossible in reality. Furthermore, the system settles into a stable equilibrium rather than reproducing the slow, continuous depletion of CD4+ T cells that leads to AIDS, and it oversimplifies biological dynamics by neglecting the influence of the immune response and cellular heterogeneity.

III. CELL-TO-CELL TRANSMISSION MODEL

To overcome the limitations of the basic viral dynamics model, particularly its inability to represent long-term progression and reservoirs, researchers have proposed several extensions. The first alternative formulation we analyze is the **cell-to-cell** transmission model (*Figure 5*).

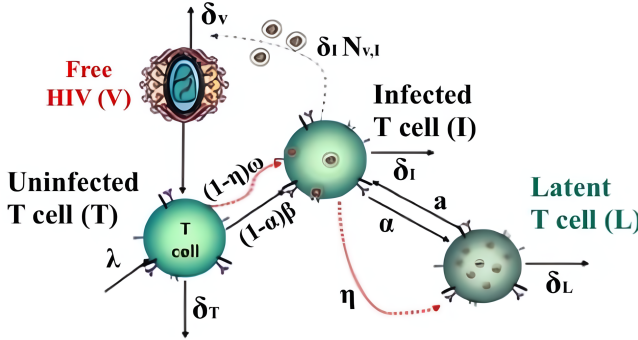


Fig. 5. The diagram shows the interaction between uninfected CD4+ T cells (T), infected T cell (I), free virus (V) and latent T cell (L), each governed by its own parameters.

A major flaw of the basic model is its failure to account for the diversity of cell populations that support viral spread, specifically chronic and latent populations. These cells act as **HIV reservoirs** and pose a major obstacle to eradication [14]. **Latent population** models describe the transition of a portion of infected cells into a latent state, where they persist for months or years, even under treatment, before potentially reactivating upon antigenic stimulation. Similar to chronic infection, latent cells arise at a rate proportional to an infection fraction α , but are characterized by a significantly lower death rate δ_L compared to actively infected cells.

The cell-to-cell transmission model builds upon these premises by introducing a **dual** transmission pathway. While the basic model considers only cell-free virus transmission, HIV can also spread directly through contact between infected and healthy cells. This mode of transmission is evolutionarily advantageous: it protects viral progeny from the extracellular environment and immune defenses, increasing the efficiency of spread by several orders of magnitude compared to cell-free dissemination [15] [16]. Crucially, this pathway influences the establishment and maintenance of the latent reservoir, thereby hindering immune clearance and reducing the effectiveness of ART.

The system is composed of four different ODEs that describe the dynamics of free virus (V) and not infected (T), actively infected (I), latent infected (L) cells. For which we need to define a list of parameters (*Table II*).

The parameters are divided between those **specific** to this model and those **inherited** from previous formulations. New parameters include ω , the cell-to-cell infection rate, and η , the fraction of cells entering latency via cell-to-cell transmission. Standard parameters shared with the basic and latent models

include the free virus infection rate β , the virus-mediated latency fraction α , the drug efficacy ϵ , the latency reactivation rate a , the production and death rates for T-cells and virus ($\lambda, \delta_T, \delta_I, \delta_L, \rho, \delta_V$).

The four ODEs that model the systems are:

$$\frac{dT}{dt} = \lambda - \delta_T T - (1 - \epsilon)\beta V T - \omega I T \quad (1)$$

$$\frac{dI}{dt} = (1 - \alpha)(1 - \epsilon)\beta V T + (1 - \eta)\omega I T + a L - \delta_I I \quad (2)$$

$$\frac{dL}{dt} = \alpha(1 - \epsilon)\beta V T + \eta\omega I T - a L - \delta_L L \quad (3)$$

$$\frac{dV}{dt} = \rho I - \delta_V V \quad (4)$$

The first equation describes the change in the number of healthy T cells over time, it tracks the production, natural death and infection of healthy T cells via both free virus and direct cell-to-cell contact.

The second equation models actively infected cells, which arise from both infection pathways and latency reactivation, balanced by natural death.

Third equation defines the **latent reservoir** (dL/dt), representing infected cells that do not produce virus. These are formed from a fraction of new infections (α and η) and are lost through reactivation (aL) or death ($\delta_L L$).

Finally, the fourth equation describes the behaviour of free viral load, driven by production from actively infected cells and cleared by the immune system.

Compared to the basic model, these equations introduce two fundamental concepts: **fate bifurcation** and **dual infection** pathway. The first term indicates how infected cells can either become inactive or latent, with probabilities α or η respectively, depending on the infection route. The second term describe how the infection depends not only on the presence of free virus ($\beta V T$), but also on the density of already infected cells ($\omega I T$).

This implies that even if therapy (ϵ) or the immune response drastically reduces free viral load ($V \approx 0$), the infection can continue to propagate and sustain itself as long as infected cells remain in contact with healthy cells. This fuels both the active and latent reservoirs (L), contributing to viral persistence despite effective suppression of free virus.

We implemented the model on Matlab to study its dynamics, both with and without ART treatment. We use *ode45*, as function for nonstiff ODEs, it assumes a continuous, deterministic system, but when viral loads or latent cell counts become very low (during ART), stochastic effects (Gillespie algorithm) become more relevant because "extinction" of the virus can only be captured in a stochastic framework.

The core of the model relies on the **Basic Reproduction Number** (R_0), which is defined as the average number of

TABLE II
Parameters for the cell-to-cell HIV Model

Parameter	Description	Value	Units/Notes
λ	T-cell production rate	10^4	$\text{cells mL}^{-1} \text{ day}^{-1}$
δ_T	Natural T-cell death rate	0.01	day^{-1}
β	Virus-to-cell transmission rate	2.4×10^{-8}	$\text{mL virion}^{-1} \text{ day}^{-1}$
ω	Cell-to-cell transmission rate	10^{-6}	$\text{mL cell}^{-1} \text{ day}^{-1}$
δ_I	Active infected cell death rate	1.0	day^{-1}
$N_{v,i}$	Viral burst size	2000	virions cell^{-1}
δ_V	Viral clearance rate	23.0	day^{-1}
a	Latency reactivation rate	0.01	day^{-1}
δ_L	Latent cell death rate	0.004	day^{-1}
α	Latency fraction (virus infection)	0.001	dimensionless
η	Latency fraction (cell-to-cell)	0.001	dimensionless
ϵ	Antiretroviral drug efficacy	0.90	dimensionless

secondary infections produced by a single infected cell in a population. In the code, R_0 is computed in this way:

$$R_0 = R_{0,\text{virus}} + R_{0,\text{cell}} = \frac{\beta T_0 \rho}{\delta_I \delta_V} + \frac{\omega T_0}{\delta_I}$$

In the simulation output R_0 is likely significantly greater than 1, which guarantees the transition from the Disease-Free Equilibrium (DFE), healthy state, to an Endemic Equilibrium (chronic infection steady-state) driven by $R_0 > 1$ (condition that remains true for all the simulations of the report).

After having defined all the parameters we need for the simulation, we start by examining the development of the illness without treatment (*Figure 6*), across a period of 200 days. This figure represents the natural history of an acute HIV infection, from which we can study the 3 subplots.

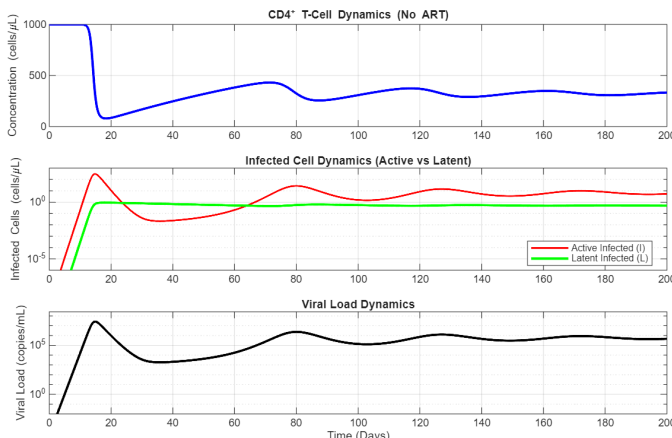


Fig. 6. **Simulation of cell-to-cell model without treatment:** The top panel tracks the T-cell population dynamics, with concentration (cells/ μL) on the y-axis and a 200 days period on the x-axis. In the second panel, the concentration of latent infected cells (green) and of active infected cells (red) is presented, with concentration (cells/ μL) as the y-axis. The last plot represents the viral load measured in copies/ mL .

The first plot represents the CD4+ dynamics, particularly the target cell population (T). Initially, the concentration is at its healthy equilibrium ($T_0 = 1000 \text{ cells}/\mu\text{L}$), where the production rate λ is balanced by the natural death rate δ_T .

Initially, the viral load and active infected cells (I) undergo an **exponential growth**. As the infection takes hold, it can be observed a significant decline in T-cells. This is caused by both direct viral infection (βVT) and cell-to-cell transmission (ωIT). The plot reaches a low point before stabilizing at a much lower, chronic level. This reflects how the virus depletes the immune system's primary defenders, leading to a new, weakened equilibrium.

The second plot, displayed on a log scale to capture the rapid expansion, tracks two populations of infected cells. The actively infected cells surge rapidly to a **high peak** during the initial infection and then **decline**. In contrast, the latent infected cells establish a much smaller but persistent reservoir that declines very slowly over time, representing a long-term viral archive in the body.

The third plot shows the concentration of free virions in the plasma, which is the most common clinical marker for HIV progression. Following infection, the viral load **explodes exponentially** to a very high peak ($10^5 - 10^6$ copies/ mL), marking the highly contagious acute phase. It then falls and stabilizes at a lower, steady level, the **viral set-point**. This set-point is maintained by a dynamic balance: new virions are produced by active cells at rate ρ_I , while being cleared by the immune system or natural decay at rate δ_V .

We then decided to analyze the development of the disease when administered the **ART** (*Figure 7*).

The image illustrates the impact of Antiretroviral Therapy (ART), introduced via the parameter ϵ (efficacy), demonstrating how the introduction of this drug efficacy parameter shifts the system from an endemic equilibrium toward a state of **viral suppression**. The first graph shows the recovery of healthy immune cells. Upon the initiation of ART, the decline in CD4+ T-cells stops and the population begins to consistently increase over time. In the Matlab script, the infection term is modified by reducing the rate of new infections by 90%: $(1 - \epsilon)\beta$. This represents the system returning toward its healthy steady state ($\approx \lambda\delta_T$). However, the recovery is not instantaneous; it is governed by the slow production rate and the presence of

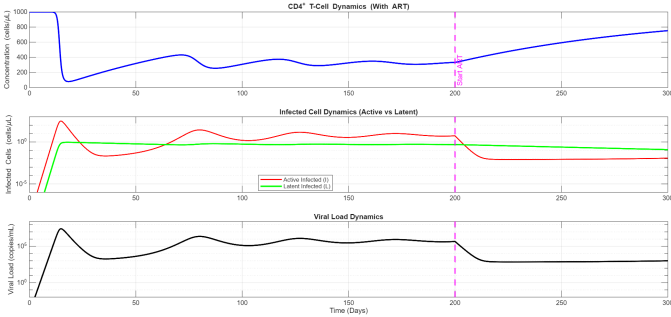


Fig. 7. **Simulation of cell-to-cell model with ART treatment:** The treatment start is defined with the dashed magenta line at day 200. The top panel tracks the T-cell population dynamics, with concentration (cells/ μ L) on y-axis and a 300 days period on x-axis. In the second panel is present the concentration of latent infected cells (green) and of active infected cells (red), with as y-axis concentration (cells/ μ L). The last plot has as y-axis the viral load measured in copies/mL.

infected cells. The fact that T-cells do not reach their original 10^6 level immediately suggests a "**residual infection**" or a new equilibrium.

Displayed on a log scale, the second plot, for infected cell dynamics, highlights the **biphasic decay** of infected populations. Actively infected cells rapidly decline after treatment starts, reflecting their short lifespan. In contrast, the latent infected cells decay at a much slower, **almost flat rate**, revealing the persistence of a long-lived viral reservoir that is not immediately eliminated by the drugs.

The viral suppression plot shows that, following the start of ART, the viral load undergoes a sharp decline, falling by several orders of magnitude. However, it does not reach zero; instead, it stays at a very low, steady state. This represents successful clinical suppression with a low level of residual virus that persists despite treatment.

IV. IMMUNE DYNAMICS MODEL

Until now, we only focused on modeling the disease itself, without taking into consideration other important factors that play a crucial role inside the development of the disease, such as the **immune response**. The immune system is in fact fundamental in the protection against pathogens. Human immunity against viruses can be categorized into two types: **cell mediated immunity** and **humoral immunity**. The former involves cytotoxic T lymphocytes (CTLs) that eliminate infected cells, by directly recognizing the viral antigen on the surface and inducing the programmed cell death [17]. While the latter, includes B cells that derive from naïve B cells produced by the thymus. When the naïve B cells encounter antigen combined with support signals from T cells, they mature and become memory and plasma cells which are respectively responsible for recall responses and for secreting high levels of plasma antibodies to attack free virions [18]. For this complex interplay between these two different levels of immunity is fundamental to be able to implement both of them in the model; to have at the end a broad view of what is realistically and biologically happening during the development of the disease.

To study and include also this response to the simulations, many models have been developed. Starting with the inclusion of CTLs in viral dynamics. In the model developed by Guo and Qiu [19] it is possible to study and model altogether the cell-mediated immunity model, the latent cells and cell-to-cell transmission. It includes in the model new parameters: p , rate of CTLs recruitment in proportion to infected cells; δ_E , death rate; m , rate of CTLs killing infected cells. The model lets us see the critical role that CTLs have in the control of HIV; but of course, one of the major limitations is that it doesn't take into account the whole response, excluding the humoral response from the model.

The first models developed by Wang and Zou [20] and Murase et al. [21] improved the basic viral dynamics model by incorporating the humoral immune response, but of course they had the same limitation as before: they didn't consider the whole immune response. The model that our review present is the one by Lin et al. [12], that considers the cell-to-cell transmission with both cellular and humoral response (Figure 8).

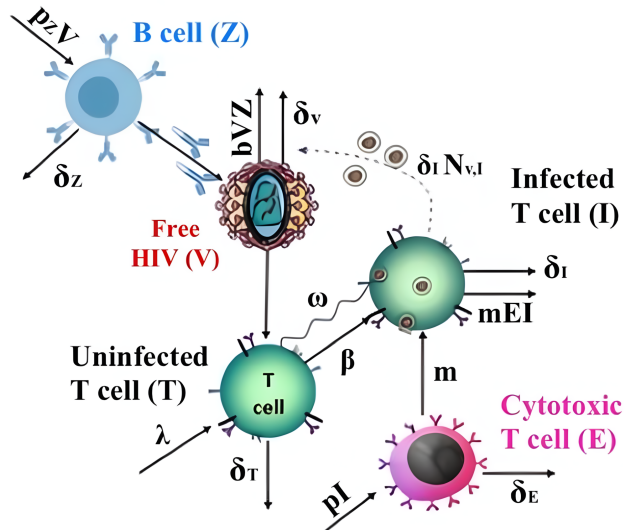


Fig. 8. The diagram shows the interaction between uninfected CD4+ T cells (T), infected T cell (I), free virus (V), cytotoxic T cell (E) and B cells (Z), each governed by its own parameters.

The new fundamental parameters that are described in the model, that can be found in (Table III) are the saturation (s), to evolve the model from the simpler ones, by assuming that the infection rates do not increase indefinitely with viral load but reflect a more **biological realistic plateau**; m and b_z parameters for active, immune-driven elimination, an advance with respect to the natural driven deaths controlled by δ_V and δ_I of other models; ρ_I , ρ_Z , δ_E , δ_Z that describe immune population dynamics, allowing it to expand and contract based on the severity of the infection.

TABLE III
Parameters for the Immune System HIV Model

Symbol	Description	Value	Units
λ	T-cell production rate	100	cells mm^{-3} day $^{-1}$
δ_T	Natural T-cell death rate	0.0046	day $^{-1}$
β	Virus-to-cell infection rate	4.8×10^{-7}	$\text{mm}^3 \text{ virion}^{-1} \text{ day}^{-1}$
ω	Cell-to-cell transmission rate	4.7×10^{-7}	$\text{mm}^3 \text{ cell}^{-1} \text{ day}^{-1}$
s	Saturation constant	0.01	$\text{mm}^3 \text{ virion}^{-1}$
δ_I	Infected cell death rate	0.008	day $^{-1}$
m	CTL neutralization rate	0.001	$\text{mm}^3 \text{ cell}^{-1} \text{ day}^{-1}$
$N_{v,i}$	Viral burst size	2000	virions cell $^{-1}$
δ_V	Viral clearance rate	0.05	day $^{-1}$
b_z	Humoral neutralization rate	0.01	$\text{mm}^3 \text{ antibody}^{-1} \text{ day}^{-1}$
p_I	CTL recruitment rate	0.002	$\text{mm}^3 \text{ cell}^{-1} \text{ day}^{-1}$
δ_E	CTL natural death rate	0.02	day $^{-1}$
p_Z	Humoral (B-cell) recruitment rate	0.0013	$\text{mm}^3 \text{ virion}^{-1} \text{ day}^{-1}$
δ_Z	Humoral natural death rate	0.12	day $^{-1}$
ϵ	Antiretroviral drug efficacy	0.90	dimensionless

This model is described by 5 differential equation:

$$\frac{dT}{dt} = \lambda - \delta_T T - \frac{(1-\epsilon)\beta VT}{1+sV} - \omega IT \quad (1)$$

$$\frac{dI}{dt} = \frac{(1-\epsilon)\beta VT}{1+sV} + \omega IT - \delta_I I - mEI \quad (2)$$

$$\frac{dV}{dt} = N_{v,i}\delta_I I - \delta_V V - b_z VZ \quad (3)$$

$$\frac{dE}{dt} = p_I IE - \delta_E E \quad (4)$$

$$\frac{dZ}{dt} = p_Z VZ - \delta_Z Z \quad (5)$$

The first equation, for modeling the uninfected T cells, characterizes the temporal evolution of the susceptible CD4+ T-cell population. It accounts for the **homeostatic production** of new cells and their subsequent loss, which occurs through natural death or the process of infection. The infection term integrates both virus-to-cell transmission (often subject to saturation) and direct cell-to-cell transmission.

The second equation focuses on infected T cells. The population size increases as healthy cells are converted through the **infection pathways**. Reductions in this population are driven by natural infected-cell death and active elimination by cytotoxic T lymphocytes (CTLs), which constitute the cell-mediated immune response.

We then study the concentration of free virions in the third equation, where viral load increases via the burst of new particles released from infected cells. While viral levels are reduced through natural decay and the humoral immune response (neutralization of free virions by B cells).

The fourth equation describes the immune response with the Cytotoxic T cells dynamics. It represents the expansion and proliferation of effector "killer" cells in direct proportion

to the abundance of infected cells, while also accounting for their natural turnover or death rate. The mathematical term that describes this behavior of elimination or killing of infected cells from Cytotoxic T cells is $-mEI$.

Finally, the last equation describes the **B cells dynamics**, for the humoral immune response. It models the recruitment and production of B cells, stimulated by the presence of free viral particles, considering also their natural rate of clearance from the system. The term that delineates this neutralization of free virions by B cells is $-b_z VZ$.

For the simulation in Matlab we solve numerically the system of ODEs over a 200-day period. We can study each plot, to define how the infection and the disease develop in the presence of the immune system without the presence of ART (*Figure 9*).

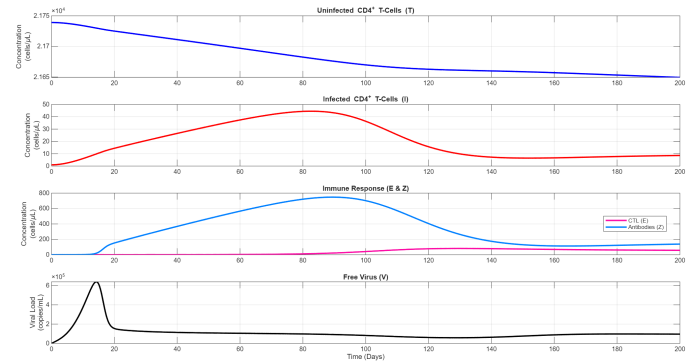


Fig. 9. **Simulation of immune model without treatment:** The top panel tracks the uninfected CD4+ T-cell, with concentration (cells/ μL) on y-axis and 200 days period on x-axis. In the second panel the concentration of infected CD4+ T-cells is presented. The third panel shows the concentration of CTL (E) (magenta) and concentration of antibodies (blue). The last plot has as y-axis the viral load measured in copies/mL.

It should be immediately noticeable a huge difference with respect to the plots that we obtained so far. Each curve is more gradual, reflecting the presence of the immune system

that contrasts the viral infection, substantiating what we expected from theoretical knowledge.

The first plot defines the population of uninfected CD4+ T-cells. It shows a **continuous decline** from its initial equilibrium. The infection rate depends both on the virus-to-cell transmission and cell-to-cell transmission. Moreover, the presence of the saturation constant prevents the collapsing of the population by limiting the rate of infection at high viral loads.

The second plot describes the behavior of infected CD4+ T-cells, with their concentration that rises steadily, with a peak around the 85th day, before beginning a **gradual decline**. The initial rise is due the abundance of uninfected targets and free viruses; while the subsequent decline is the direct result of the cell-mediated immune response.

The immune response plot shows the dynamics of the immune system components. For the **antibodies** can be observed a rapid expansion starting around day 15, as they need to respond to the initial burst of free virus. Whereas, for the **CTLs** we can notice a slower but sustained recruitment, following the persistent population of infected cells.

Finally, the last graph represents the free virus. We can observe an acute peak around day 15, with viral load exceeding 6×10^5 copies/mL, followed by a rapid crash, driven by humoral immunity and natural clearance rate. This leads to the establishment of a stable, lower-level viremia and means that the immune system has reached a **balance** with the viral production from surviving infected cells.

We can then analyze the simulation of the same model studied during 300 days, with the start of ART treatment at day 200, demonstrating the effect of pharmacodynamic intervention on the disease development (*Figure 10*).

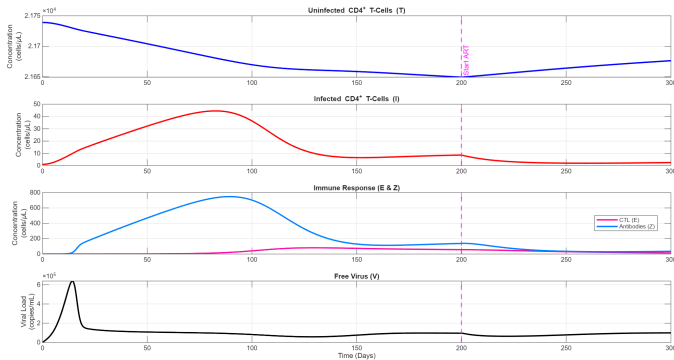


Fig. 10. Simulation of immune model with ART treatment: The treatment start is defined with the dashed magenta line at day 200. The top panel tracks the uninfected CD4+ T-cell, with concentration (cells/ μ L) on y-axis and a 300 days period on x-axis. In the second panel the concentration of infected CD4+ T-cells is presented (cells/ μ L). The third panel shows the concentration of CTL (E - magenta) and concentration of antibodies (Z - blue). The last plot has as y-axis the viral load measured in copies/mL.

Comparing the graph resulting from this simulation and those from previous simulations, we can immediately appreciate the great difference in the decrease of the infected cells. When ART is introduced in a system with an already active immune system, the starting levels of infected cells and viral load are much smaller, compared to the simulations without immune

activity. For this reason, we can notice a smaller decrease in absolute terms (a more **controlled** and **gradual suppression** rather than an abrupt one), that still represents the more realistic response to the start of the treatment, as clinically observed. This behavior aligns with the expected dynamics in a host with preserved immune function.

The first plot shows the uninfected CD4+ T-cells in the first 200 days, where the population exhibits a **slow but progressive decline**, while after the initiation of the therapy, the infection rate is significantly reduced, resulting in a visible **recovery** of the healthy T-cell count.

The behavior of the infected cells is represented in the second plot, where it can be seen that the treatment leads to a blockage of the formation of new infected cells from the uninfected pool, while the existing infected population decays at its natural and immune-driven death rates.

In the third plot we can appreciate the **immune response behavior**. In fact, after the start of the treatment we can see that as the concentration of infected cells and free viruses decreases, the stimulus for immune proliferation is lost leading to the contraction of the immune population.

Finally, the last plot shows the free virus load that undergoes a **multi-phasic decay** toward the detection limit after the starting of the treatment. The rapid decline is driven by the termination of production of new virions and the high clearance rate of free particles.

By simulating the complex interplay between viral replication and host immune responses, these models provide a framework to identify the most impactful biological parameters and predict long-term clinical outcomes. Rather than viewing infection as a static state, the modeling approach reveals a **dynamic "set point"** where the virus and the immune system exist in a delicate, shifting equilibrium.

One of the most significant insights gained from these models is the understanding of how the dual branches of the immune system collaborate to restrict viral spread. Simulations demonstrate that while individual responses are helpful, it is the **combined** pressure of cytotoxic T cells and neutralizing antibodies that achieves the lowest stable viremia during the chronic phase. Furthermore, the inclusion of features such as cell-to-cell transmission and saturation effects highlights how the virus utilizes mechanical advantages to evade host defenses, offering a plausible explanation for why natural immunity alone rarely achieves eradication.

V. COMPLEX MODEL

The final model proposed is the most intricate one, but offers superior **biological realism**. It aims to replicate the entire course of the infection, from the acute stage to the development of AIDS. It represents 13 distinct **subclasses** of cells, distinguishing between HIV-specific and non-specific T-cells, as well as non-effector and effector populations. The model incorporates thymic development (including thymic infection) and accounts for viral tropism, simulating the shift from macrophage-tropic to T-cell-tropic variants. Furthermore, it integrates the dynamics of neutralizing antibodies and infected

macrophages, modeling the interaction between the virus and the immune system. The schematic representation of the model is illustrated in *Figure 11*.

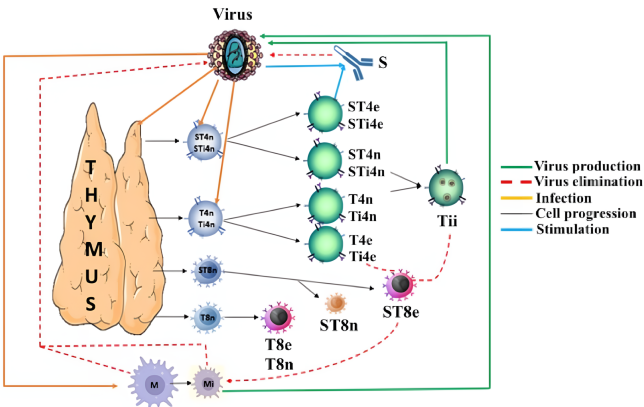


Fig. 11. **Complex model diagram.** The image illustrates the interactions between HIV and specific/non-specific T-cells (both T4 and T8), macrophages, and antibodies. The model also considers thymus' role.

The model introduces a significant number of parameters, the list with the respective values is presented in *Table IV*. Key additions compared to basic models include distinct proliferation rates for specific (ρ) versus non-specific (r) T-cells, and time-dependent functions for viral infectivity and antibody neutralization to simulate biological adaptation.

The mathematical framework consists of a system of 16 ODEs, which can be divided into the following sections:

- HIV-specific T4 cells (eq 1-4)
- Non-specific T4 cells (eq 5-8)
- T8 cells (eq 9-12)
- Actively infected Tii cells (eq 13)
- Antibodies (eq 14)
- Infected macrophages (eq 15)
- Free virus (eq 16)

$$\frac{d\tilde{T}_{4n}}{dt} = \nu fs \left(1 - \frac{e(1-\epsilon)V}{c_1 + V} \right) + (1-\varphi) \frac{\rho_4 V}{c_2 + V} \tilde{T}_{4n} - k_v(1-\epsilon) \frac{V}{c_2 + V} \tilde{T}_{4n} - \mu_{4n} \tilde{T}_{4n} \quad (1)$$

$$\frac{d\tilde{T}_{4e}}{dt} = \varphi \frac{\rho_4 V}{c_2 + V} \tilde{T}_{4n} - k_v(1-\epsilon) \frac{V}{c_2 + V} \tilde{T}_{4e} - \mu_{4e} \tilde{T}_{4e} \quad (2)$$

$$\frac{d\tilde{T}_{4n}^i}{dt} = \nu fs \frac{e(1-\epsilon)V}{c_1 + V} + [(1-\varphi)(1-p) - p] \frac{\rho_4 V}{c_2 + V} \tilde{T}_{4n}^i + k_v(1-\epsilon) \frac{V}{c_2 + V} \tilde{T}_{4n} - (k_8 \delta \tilde{T}_{8e} + \mu_{4n}^i) \tilde{T}_{4n}^i \quad (3)$$

$$\frac{d\tilde{T}_{4e}^i}{dt} = \varphi(1-p) \frac{\rho_4 V}{c_2 + V} \tilde{T}_{4n}^i + k_v(1-\epsilon) \frac{V}{c_2 + V} \tilde{T}_{4e} - (k_8 \delta \tilde{T}_{8e} + \mu_{4e}^i) \tilde{T}_{4e}^i \quad (4)$$

These equations govern the dynamics of the HIV-specific CD4+ T cell population, which is subdivided into **healthy** (eq 1-2) and latently **infected** (eq 3-4) pools, as well as **non-effector** and **effector** states. The healthy specific non-effector

pool ($ST4n$) is supplied by the **thymus**, where a fraction of cells may be infected before release, and proliferates in response to viral stimulation at rate ρ_4 . A portion of these proliferating cells differentiates into effectors ($ST4e$), while others remain in the memory/naive pool. Both subsets are depleted by viral infection (k_v), which moves them into the corresponding latently infected compartments ($ST4ni$, $ST4ei$). The infected populations are removed through natural death or immune recognition by cytotoxic T8 cells (k_8), the latter being reduced by a factor δ due to the latency of the infection.

$$\begin{aligned} \frac{dT_{4n}}{dt} &= (1-\nu)fs \left(1 - \frac{e(1-\epsilon)V}{c_1 + V} \right) + (1-\varphi)r_4 T_{4n} \\ &\quad - k_v(1-\epsilon) \frac{V}{c_2 + V} T_{4n} - \mu_{4n} T_{4n} \end{aligned} \quad (5)$$

$$\frac{dT_{4e}}{dt} = \varphi r_4 T_{4n} - k_v(1-\epsilon) \frac{V}{c_2 + V} T_{4e} - \mu_{4e} T_{4e} \quad (6)$$

$$\begin{aligned} \frac{dT_{4n}^i}{dt} &= (1-\nu)fs \frac{e(1-\epsilon)V}{c_1 + V} + [(1-\varphi)(1-p) - p]r_4 T_{4n}^i \\ &\quad + k_v(1-\epsilon) \frac{V}{c_2 + V} T_{4n} - (k_8 \delta \tilde{T}_{8e} + \mu_{4n}^i) T_{4n}^i \end{aligned} \quad (7)$$

$$\begin{aligned} \frac{dT_{4e}^i}{dt} &= \varphi(1-p)r_4 T_{4n}^i + k_v(1-\epsilon) \frac{V}{c_2 + V} T_{4e} \\ &\quad - (k_8 \delta \tilde{T}_{8e} + \mu_{4e}^i) T_{4e}^i \end{aligned} \quad (8)$$

Equations 5-8 describe the **non-specific** T4 cells, which provide the general pool of CD4+ targets for the virus but do not specifically respond to HIV antigens. The structure of these equations mirrors that of the specific cells, with supply from the thymus and removal via infection and death. The crucial difference lies in the proliferation term: unlike specific cells which respond to the virus, non-specific T4 cells proliferate at a **constant background rate** (r_4) driven by environmental antigens. Consequently, their population dynamics are not directly coupled to the viral load in terms of expansion, but they serve as a major reservoir for latent infection.

$$\frac{d\tilde{T}_{8n}}{dt} = \nu(1-f)s + (1-\varphi)R\tilde{T}_{8n} - \mu_{8n}\tilde{T}_{8n} \quad (9)$$

$$\frac{d\tilde{T}_{8e}}{dt} = \varphi R\tilde{T}_{8n} - \mu_{8e}\tilde{T}_{8e} \quad (10)$$

$$\frac{dT_{8n}}{dt} = (1-\nu)(1-f)s + (1-\varphi)r_8 T_{8n} - \mu_{8n} T_{8n} \quad (11)$$

$$\frac{dT_{8e}}{dt} = \varphi r_8 T_{8n} - \mu_{8e} T_{8e} \quad (12)$$

The T8 cell populations (CD8+) are modeled in equations 9-12, split into HIV-specific (ST8) and non-specific pools. Unlike T4 cells, T8 cells in this model are assumed **not to be infected** by the virus after leaving the thymus, so there are no infection terms removing cells from these healthy pools. The specific T8 cells (eq 9-10) are the **cytotoxic effectors** responsible for killing infected cells, so their proliferation (R)

TABLE IV
Parameters for the Complex HIV Model

Parameter	Description	Value	Units/Notes
a_M	Macrophage compartment conversion	0.03	–
a_T	T cell compartment conversion	0.06	–
c_1	Half saturation for V in thymus	616.6	particles mm ⁻³
c_2	Half saturation for V in blood	1000	particles mm ⁻³
δ	Reduced immune recognition coefficient	0.001	–
f	Fraction of T4 cells (vs. T8)	0.524	–
k_8	Rate T_{8e} removes infected cells	2.5	mm ³ cell ⁻¹ day ⁻¹
k_m	Rate macrophages remove virus	60	particles day ⁻¹
M_{total}	Total macrophage density	360	cells mm ⁻³
μ_{Ab}	Death rate of antibodies	0.023	day ⁻¹
μ_M	Macrophage death rate	0.1	day ⁻¹
μ_{4e}	Death rate of T4 effectors	0.015	day ⁻¹
μ_{4n}	Death rate of T4 non-effectors	0.005	day ⁻¹
μ_{8e}	Death rate of T8 effectors	0.018	day ⁻¹
μ_{8n}	Death rate of T8 non-effectors	0.006	day ⁻¹
μ_{ii}	Death rate of actively infected cells	0.57	day ⁻¹
μ_V	Viral clearance rate	3.0	day ⁻¹
N	Viral burst size	850	virions cell ⁻¹
p	Probability of latent activation	0.03	–
ϕ	Fraction of T cells differentiating	0.64	–
p_{im}	Virus production by infected macrophages	32	particles cell ⁻¹ day ⁻¹
ρ_{Ab}	Max antibody production rate	1.55×10^5	molecules
ρ_4	Specific T4 proliferation rate	1.98	day ⁻¹
ρ_8	Specific T8 proliferation rate	0.36	mm ³ cell ⁻¹ day ⁻¹
r_4	Non-specific T4 proliferation rate	0.0097	day ⁻¹
r_8	Non-specific T8 proliferation rate	0.0091	day ⁻¹
ν	ST4 / total T4 ratio in thymus	0.001	–
\bar{s}	T cell flow from thymus to blood	6.09	cells mm ⁻³ day ⁻¹
\bar{k}_v	Base rate of T4 infection	0.5	mm ³ virion ⁻¹ day ⁻¹
\bar{e}	Base rate of thymic infection	0.064	–
\bar{k}_{vm}	Base rate of macrophage infection	1.19	day ⁻¹
\bar{k}_{Ab}	Base antibody removal rate	2.0×10^{-7}	–
A	Subject age	36	years
ϵ	ART efficacy	0.9	–

is stimulated directly by the presence of infected cells. The non-specific T8 cells (eq 11-12) proliferate at a constant rate r_8 and serve mainly to track the overall CD8 count and the T4/T8 ratio.

$$\frac{dT_{ii}}{dt} = p \left(r_4 T_{4n}^i + \frac{\rho_4 V}{c_2 + V} \tilde{T}_{4n}^i \right) - (k_8 \tilde{T}_{8e} + \mu_{ii}) T_{ii} \quad (13)$$

This equation describes the actively producing infected T cells (T_{ii}). They are generated from the activation of latently infected T4 cells (both specific and non-specific) with a probability p . These cells are the **primary source of viral bursting** from T-cells and are removed rapidly from the system either by specific cytotoxic T8 killing or by virus-induced cell death (μ_{ii}).

$$\frac{dS}{dt} = \rho_{Ab} (\tilde{T}_{4e} + \tilde{T}_{4e}^i) \frac{V}{c_2 + V} - k_{Ab} VS - \mu_{Ab} S \quad (14)$$

Equation 14 tracks the concentration of specific neutralizing **antibodies** (S). Their production is dependent on the help provided by specific T4 effector cells ($ST4e$) in the presence of viral stimulation. The antibody population is depleted as it binds to free virus to form antigen-antibody complexes (represented by the term $-k_{Ab} VS$), effectively neutralizing the virus, and by natural decay.

$$\frac{dM_i}{dt} = k_{vm} (1 - \epsilon) \frac{V}{c_2 + V} (M - M_i) - (k_8 \delta \tilde{T}_{8e} + \mu_M) M_i \quad (15)$$

The dynamics of infected **macrophages** are described in equation 15. Macrophages are infected by free virus at a rate k_{vm} , which evolves over time to reflect viral tropism changes. Unlike T cells which burst and die, infected macrophages persist as a long-term reservoir, producing virus continuously until they are removed by cytotoxic T8 cells (with reduced efficiency δ) or die naturally.

$$\frac{dV}{dt} = \frac{p_{im}}{a_M} M_i + \frac{N\mu_{ii}}{a_T} T_{ii} - k_m \frac{V}{c_2 + V} \frac{M_{total}}{a_M} - \frac{e(t)(1-\epsilon)V}{c_1 + V} s(t) \quad (16)$$

$$- \frac{k_v(t)(1-\epsilon)}{a_T} \frac{V}{c_2 + V} (\tilde{T}_{4n} + \tilde{T}_{4e} + T_{4n} + T_{4e}) - k_{Ab}(t)SV - \mu_V V \quad (17)$$

The final equation accounts for the **free viral load** (V). Virus is produced by two sources: the continuous release from infected macrophages (p_{im}) and the lytic bursting of actively infected T cells ($N\mu_{ii}$). Viral clearance is mediated by four mechanisms: removal by macrophages (k_m), uptake during the infection of new cells (both thymocytes and circulating T4 cells), neutralization by antibodies (k_{Ab}), and natural decay (μ_V). The terms include scaling factors (a_M, a_T) to account for the differences between blood volume and total body distribution.

The simulation of the untreated model faithfully reproduces the classic multi-phasic progression of HIV infection (Figure 12).

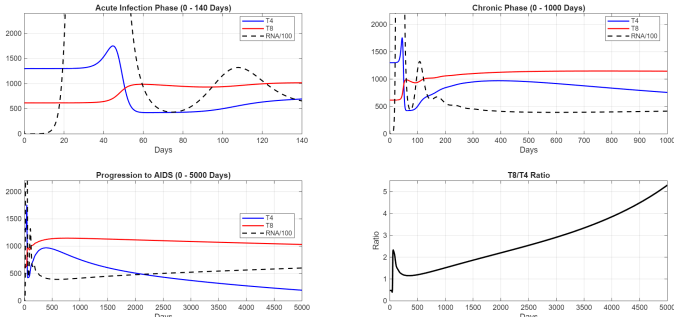


Fig. 12. Simulation of untreated HIV with complex model. The model reproduces the characteristic triphasic progression, including the acute-phase double viral peak (black dashed) and the eventual collapse of CD4+ T cells (blue) due to viral tropism switching and thymic exhaustion. The CD8+ T cell response (red) initially controls infection but ultimately fails, leading to AIDS as indicated by the collapsing T8/T4 ratio.

The **acute phase** (approximately days 0-100) is distinguished by a characteristic **double viral peak** phenomenon. This key feature arises from the model's explicit separation of cellular compartments. The first, high-amplitude peak (reaching approximately 1.55×10^4 viral particles) corresponds to the rapid saturation of the macrophage reservoir and the infection of the initially susceptible T-cell fraction. The second peak (approximately 1.25×10^3 viral particles) is driven by a viral

tropism switch, whereby the virus evolves to efficiently target the larger circulating T-cell compartment.

Following this acute phase, the system enters a prolonged period of **clinical latency**, characterized by a **quasi-steady viral concentration** in which replication is constrained by HIV-specific cytotoxic T8 cells and neutralizing antibodies. This equilibrium, however, is inherently **unstable**. After several years, a shift in viral phenotype combined with thymic exhaustion overwhelms immune control, leading to the collapse of the specific T8 response and a rapid decline in the T4 population, marking the onset of **AIDS**.

The application of antiretroviral therapy (ART) is simulated by introducing a drug efficacy parameter $\epsilon = 0.9$, corresponding to a 90% inhibition of viral replication, beginning at day 300, shortly after resolution of the acute phase (Figure 13).

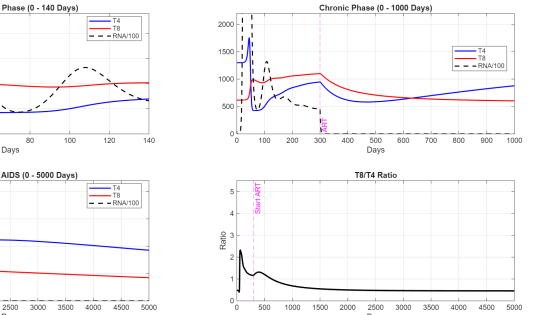


Fig. 13. Simulation of treated HIV with complex model. Intervention at day 300 (magenta line) decouples viral load (black dashed) from host dynamics, inducing exponential viral decay. This suppression allows for the robust recovery of the CD4+ T cell population (blue) and the preservation of specific immune memory, stabilizing the CD8/CD4 ratio and preventing disease progression.

The effect on system dynamics is **immediate**: the viral load (V) effectively decouples from host cell populations and undergoes exponential decay to near-undetectable levels. Importantly, the simulations demonstrate a functional recovery of the immune system. With the viral burden suppressed, the T4 cell population rebounds through sustained thymic output and homeostatic proliferation. In contrast to the untreated scenario, the CD4/CD8 ratio **stabilizes** and HIV-specific immune memory is **preserved**, maintaining the subject in a chronic, asymptomatic state and preventing progression to AIDS.

Overall, the proposed model provides a high-fidelity representation of HIV pathogenesis by extending beyond classical target-cell to virus frameworks. By incorporating distinct cellular subsets, thymic dynamics and adaptive mechanisms such as viral tropism switching, it successfully reproduces complex clinical phenomena including the acute-phase double viral peak and the eventual failure of T8-mediated immune control.

VI. CONCLUSIONS

The comparative analysis of within-host HIV models highlights that disease progression is fundamentally dictated by the non-linear interplay between viral replication, cellular availability and host immunity. The Basic Viral

Dynamics Model, utilizing the mass-action infection term $(1 - \epsilon)\beta VT$, successfully captures the initial viral burst and the establishment of a chronic set-point, yet it fails to reproduce the biphasic decay observed under ART. This limitation is addressed by the Cell-to-Cell Transmission Model, which incorporates a latent reservoir (L) and a direct infection pathway (ωIT). The discovery that latent cells possess a significantly lower death rate (δ_L) than actively infected cells (δ_I) explains the long-term viral persistence that renders complete eradication impossible.

Furthermore, the Immune Dynamics Model reveals that a biologically realistic plateau in infection is only achieved through the introduction of a saturation constant (s), which prevents the total collapse of CD4+ T-cell populations at high viral loads. The model identifies that the combined recruitment of cytotoxic T lymphocytes (CTLs) at rate p_1 and the neutralization of free virions by B cells (b_z) are the primary drivers of clinical stability during the chronic phase.

Finally, the Complex Model demonstrates that integrating thymic development and viral tropism switching is essential for replicating the triphasic progression of infection. Specifically, the explicit separation of macrophage (M_i) and T-cell (T_{ii}) compartments within a 16-ODE framework allows for the reproduction of the characteristic "double viral peak" during the acute phase. Collectively, these findings suggest that while ART facilitates robust immune reconstitution by blocking replication, the virus's ability to evade host defenses through cellular heterogeneity and mechanical advantages necessitates advanced modeling to predict long-term outcomes.

VII. SUPPLEMENTARY MATERIAL

All the Matlab implementations done for each model can be found in the GitHub repository:

<https://github.com/Catt-Git/Mathematical-Modeling-and-Simulation>

REFERENCES

- [1] World Health Organization, "Hiv data and statistics," <https://www.who.int/teams/global-hiv-hepatitis-and-stis-programmes/hiv-strategic-information/hiv-data-and-statistics>, 2024, accessed January 2, 2026.
- [2] S. G. Deeks, J. Overbaugh, A. Phillips, and S. Buchbinder, "Hiv infection," *Nature Reviews Disease Primers*, vol. 1, no. 1, 2015.
- [3] E. O. Freed, "Hiv-1 assembly, release and maturation," *Nature Reviews Microbiology*, vol. 13, no. 8, pp. 484–496, 2015.
- [4] O. Sued and T. M. Grossi, *Pathophysiology of HIV and strategies to eliminate AIDS as a public health threat*, 2023, pp. 339–376.
- [5] R. Balasubramanian, "Immune control of hiv," *Journal of Life Sciences (Westlake Village, Calif)*, vol. 1, no. 1, 2019, accessed January 2, 2026.
- [6] D. R. Burton and J. R. Mascola, "Antibody responses to envelope glycoproteins in hiv-1 infection," *Nature Immunology*, vol. 16, no. 6, pp. 571–576, 2015.
- [7] A. L. Hill, D. I. S. Rosenbloom, M. A. Nowak, and R. F. Siliciano, "Insight into treatment of hiv infection from viral dynamics models," *Immunological Reviews*, vol. 285, no. 1, pp. 9–25, 2018.
- [8] L. Marchetti, C. Priami, and V. H. Thanh, *Simulation Algorithms for Computational Systems Biology*, 1st ed., ser. Texts in Theoretical Computer Science. An EATCS Series, M. Henninger, J. Hromkovič, M. Nielsen, G. Rozenberg, and A. Salomaa, Eds. Springer, 2017. [Online]. Available: <https://link.springer.com/book/10.1007/978-3-319-63113-4>
- [9] A. V. Rodriguez, N. Velez, S. Girish, I. F. Trocóniz, and J. S. Feigelman, "Modeling the interplay between viral and immune dynamics in hiv: A review and mrgsolve implementation and exploration," *Clinical and Translational Science*, vol. 18, no. 2, pp. e70 160–e70 160, 2025.
- [10] M. A. Nowak and R. M. May, *Virus Dynamics: Mathematical Principles of Immunology and Virology*. Oxford University Press, 2000.
- [11] X. Wang, S. Tang, X. Song, and L. Rong, "Mathematical analysis of an hiv latent infection model including both virus-to-cell infection and cell-to-cell transmission," *Journal of Biological Dynamics*, vol. 11, no. sup2, pp. 455–483, 2016.
- [12] J. Lin, R. Xu, and X. Tian, "Threshold dynamics of an hiv-1 model with both viral and cellular infections, cell-mediated and humoral immune responses," *Mathematical Biosciences and Engineering*, vol. 16, no. 1, pp. 292–319, 2019.
- [13] F. Wasserstein-Robbins, "A mathematical model of hiv infection: Simulating t4, t8, macrophages, antibody, and virus via specific anti-hiv response in the presence of adaptation and tropism," *Bulletin of Mathematical Biology*, vol. 72, no. 5, pp. 1208–1253, 2010.
- [14] H. Koppensteiner, R. Brack-Werner, and M. Schindler, "Macrophages and their relevance in human immunodeficiency virus type I infection," *Retrovirology*, vol. 9, no. 1, p. 82, 2012. [Online]. Available: <https://doi.org/10.1186/1742-4690-9-82>
- [15] K. D. Pedro, A. J. Henderson, and L. M. Agosto, "Mechanisms of HIV-1 cell-to-cell transmission and the establishment of the latent reservoir," *Virus Research*, vol. 265, pp. 115–121, May 2019. [Online]. Available: <https://doi.org/10.1016/j.virusres.2019.03.014>
- [16] P. Zhong, L. M. Agosto, A. Ilinskaya, B. Dorjbal, R. Truong, D. Derse, P. D. Uchil, G. Heidecker, and W. Mothes, "Cell-to-cell transmission can overcome multiple donor and target cell barriers imposed on cell-free HIV," *PLOS ONE*, vol. 8, no. 1, p. e53138, 2013. [Online]. Available: <https://doi.org/10.1371/journal.pone.0053138>
- [17] "How cytotoxic t cells release their dying targets," *Nature Immunology*, vol. 24, pp. 1413–1414, 2023. [Online]. Available: <https://doi.org/10.1038/s41590-023-01576-0>
- [18] Q. Le Hingrat, I. Sereti, A. L. Landay, I. Pandrea, and C. Apetrei, "The hitchhiker guide to CD4+ T-cell depletion in lentiviral infection: A critical review of the dynamics of the CD4+ T cells in SIV and HIV infection," *Frontiers in Immunology*, vol. 12, p. 695674, 2021. [Online]. Available: <https://doi.org/10.3389/fimmu.2021.695674>
- [19] T. Guo and Z. Qiu, "The effects of CTL immune response on HIV infection model with potent therapy, latently infected cells and cell-to-cell viral transmission," *Mathematical Biosciences and Engineering*, vol. 16, no. 6, pp. 6822–6841, 2019. [Online]. Available: <https://doi.org/10.3934/mbe.2019341>
- [20] S. Wang and D. Zou, "Global stability of in-host viral models with humoral immunity and intracellular delays," *Applied Mathematical Modelling*, vol. 36, no. 3, pp. 1313–1322, 2012. [Online]. Available: <https://doi.org/10.1016/j.apm.2011.07.086>
- [21] A. Murase, T. Sasaki, and T. Kajiwara, "Stability analysis of pathogen-immune interaction dynamics," *Journal of Mathematical Biology*, vol. 51, no. 3, pp. 247–267, 2005. [Online]. Available: <https://doi.org/10.1007/s00285-005-0321-y>